DTU Library

Mixed-Mode Oscillations Due to a Singular Hopf Bifurcation in a Forest Pest Model

Brøns, Morten; Desroches, Mathieu; Krupa, Martin

Published in:
Mathematical Population Studies

Link to article, DOI:
10.1080/08898480.2014.925344

Publication date:
2015

Document Version
Peer reviewed version

Mixed-mode oscillations due to a singular Hopf bifurcation in a forest pest model

M. Brøns[a], M. Desroches[b], M. Krupa[b,c]

[a]*Department of Mathematics, Technical University of Denmark, Building 303S, 2800 Kgs. Lyngby, Denmark*
[b]*INRIA Paris-Rocquencourt Research Centre, Domaine de Voluceau, Rocquencourt BP 105, 78153 Le Chesnay cedex, France*
[c]*Corresponding author. E-mail: maciej.p.krupa@gmail.com*

Abstract

We consider the dynamics of a three-variable model for forest pest proposed by Rinaldi and Muratori (Theor. Popul. Biol. **41**:26–43, 1990.) The model divides the tree population into young and old trees, as the pest mainly feeds on the old trees. This gives rise to a three timescale structure where the pest grows on a fast scale, the young trees on an intermediate scale, and the old trees on a slow scale. Canard explosions of limit cycles and existence of mixed mode oscillations have previously been identified in the model, and it has been proposed that the mixed mode oscillations are organized by a folded node singularity. We show that the model indeed has a folded node, but that this is not the key to understanding the mixed mode oscillations. Rather, a singular Hopf bifurcation is present which organizes a transition from a stable steady state to relaxation oscillations which is much more complicated than the folded node scenario. We find numerically period doublings and saddle-node bifurcations leading to isolas of periodic solutions in a bifurcation structure consistent with a singular Hopf bifurcation.

Keywords: forest pest model · slow-fast systems · canards · mixed-mode oscillations · singular Hopf bifurcation

1. Introduction

Outbreaks of the spruce budworm *Choristoneura fumiferana* have been recorded regularly in the eastern United States since the early 19th century. The budworms mainly damage balsam fir and spruce, and the outbreaks have severe economical consequences for the forest industry [19]. A population dynamics model for the interaction between trees and budworms was first proposed by Ludwig *et al.* [21] who found relaxation oscillations in the system: The populations evolve slowly in quasi-equilibrium states, briefly interrupted by periods of fast dynamics corresponding to budworm outbreaks. Since the budworm population develops on a much faster scale than the trees, the model has an inherent slow-fast structure where this kind of dynamics is expected. Relaxation oscillations are also observed in other forest pest models, e.g. [1, 4, 8, 12, 22, 24].

Here we study a three variable forest pest model proposed by Rinaldi and Muratori [24]. The population of trees is age-structured into young trees and old trees to capture that the pest mainly feeds on the old trees. In dimensionless variables the equations are

$$\dot{x} = a_1 y - a_2 x - a_3 \frac{xz}{a_4 + x}, \tag{1}$$

$$\delta \dot{y} = a_5 x - (a_6 (x - a_7)^2 + a_8 + \delta a_1) y, \tag{2}$$

$$\varepsilon \dot{z} = \left(-a_9 - a_{10} z - \frac{a_{11}}{a_{12} + z} + a_{13} \frac{x}{a_4 + x} \right) z, \tag{3}$$

where x is the population of old trees, y is the population of young trees and z is the pest population. The time scale for the old trees are taken as unity while δ and ε are the time scales of young trees and pest, respectively. For further details on the biological contents of the model, see [24].

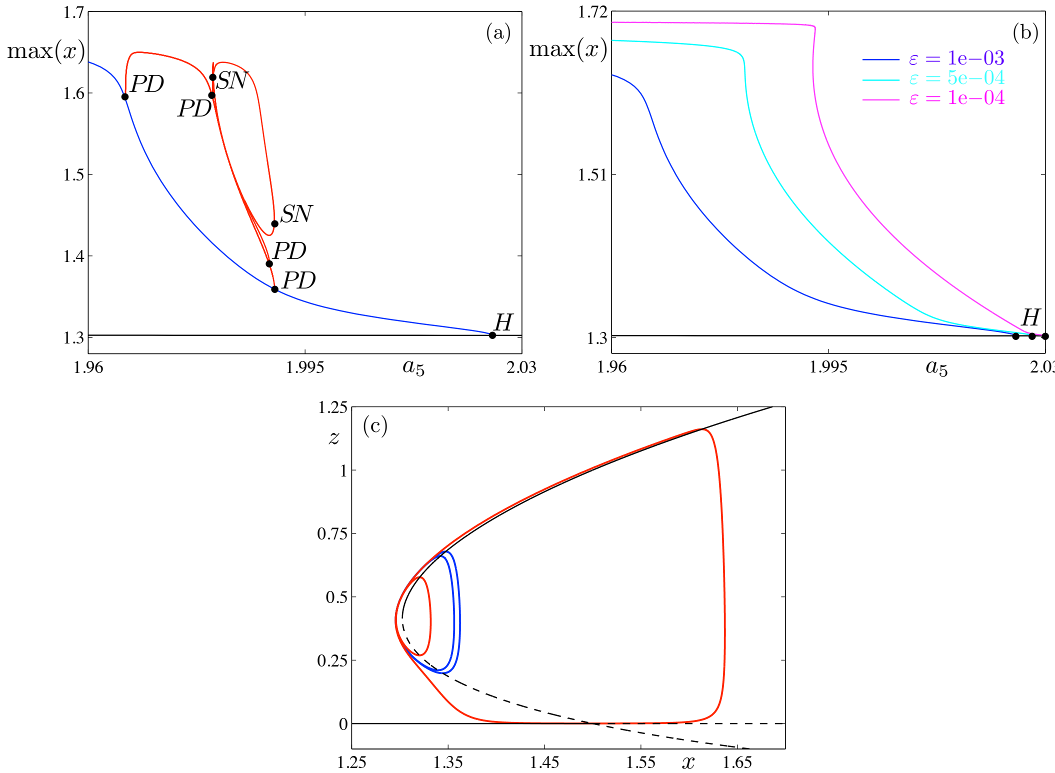

Figure 1: Panel (a) displays the bifurcation diagram of the forest pest model (1)–(3) in parameter a_5 for $\delta = 0.3$. The curve of equilibria is shown in black; the maximum in x along the branch of limit cycles is shown in blue; period-doubled branches are shown in red as well as an isola of MMOs; black dots indicate Hopf (H), period-doubling (PD) as well as saddle-node (SN) bifurcations encountered during the computation. Panel (b) shows the same branch of limit cycles computed with three different decreasing values of ε: ε = 1e−03, ε = 5e−04 and ε = 1e−04, respectively. This illustrate the explosive aspect of the branch when ε get closer to the singular limit. Panel (c) shows a period-doubled limit cycle (blue) for $a_5 \approx 1.990$ and 1^1 MMO (red) for $a_5 \approx 1.976$, along the period-doubled branch displayed in panel (a), in projection onto the (x, z)-space. The projection of the critical manifold is shown represented with its attracting (solid) and repelling (dashed) branches.

Note that system (1)-(3) has special structure given by the presence of invariant plane $\{z = 0\}$ and the presence of an invariant line $\{x = y = 0\}$. From the modeling point of view the relevant part of the space is the invariant halfspace $\{z > 0\}$, corresponding to the condition that the pest population is always positive. In the aspect of the presence of invariant spaces system (1)-(3) is similar to systems with symmetry, in which invariant spaces, and especially invariant hyperplanes often play an important role in organizing the dynamics. The role of the invariant plane for (1)-(3) will be explained in more detail in section 2.

Rinaldi and Muratori [24] consider the natural case $\varepsilon \ll \delta \ll 1$. Based on singular perturbation theory, a number of inequalities involving the parameters which guarantee the existence of a relaxation oscillations are derived. Brøns and Kaasen [6] considered the model for a fixed small ε in the limit $\delta \to 0$. Here Fenichel theory [11] allows a reduction to a two-dimensional system on an attracting invariant manifold close to $\dot{y} = 0$. It is shown that the reduced system has a *canard explosion*. When a parameter is varied through a Hopf bifurcation a limit cycle is created and experiences a rapid growth of amplitude and period to a relaxation oscillation over a very short parameter interval. Biologically, the combination of a Hopf bifurcation and a canard explosion corresponds to the transition from an infested equilibrium to a periodic state with budworm outbreaks.

The canard analysis is only valid for δ sufficiently small. As δ is increased the two-dimensional invariant manifold breaks down allowing for three-dimensional Mixed Mode Oscillations (MMOs), that is, limit cycles with long periods that change between small and large oscillations as shown in Figure 1(c).

MMOs are known to occur in systems with folded singularites [7]. We will show that a folded node is present in the system (1)–(3), but for the parameters considered in [6] it is not the organizing feature of the MMOs. Rather, a singular Hopf bifurcation [16, 17] is the singularity determining the dynamics. We analyze numerically the bifurcation structure of the MMOs and show that it is consistent with a singular Hopf bifurcation and more complex than what would be expected from a folded node scenario.

In what follows, we keep the same set of parameter values as in [6], that is, all the a_k equal to 1 except $a_2 = 0.2$, $a_3 = 7$, $a_{11} = 2$ and $a_{13} = 5$, and we fix $\varepsilon = 0.001$. The remaining two parameters, a_5 and δ, will be varied and considered as bifurcation parameters.

The rest of the paper is organized as follows. In section 2 we discuss some unusual features of system (1)-(3). In section 3, we present a numerical bifurcation analysis of the model, highlighting the structure of branches of periodic solutions in parameter space and, in particular, the region of MMOs in the (a_5, δ)-plane. In section 4, we focus on the dynamics in the fold region and show that the parameter regime considered, and the MMOs observed, correspond to the singular Hopf bifurcation scenario. Finally we conclude in section 5 and propose some avenues for future work.

2. Special features of system (1)-(3)

In this section we highlight some features of system (1)-(3) that distinguish from other systems possessing MMOs.

Equations (1)–(3) define a slow-fast dynamical system with two slow variables, x and y, and one fast variable z. The critical manifold S of this system is defined as the fast nullsurface; it is given by the equation

$$S := \left\{ \left(-a_9 - a_{10} z - \frac{a_{11}}{a_{12} + z} + a_{13} \frac{x}{a_4 + x} \right) z = 0 \right\}. \tag{4}$$

It follows that S is the union of a folded surface C and the plane $\Pi := \{z = 0\}$ with C defined by

$$C := \left\{ x = \varphi(z) = \frac{a_4(a_9 + a_{10} z + \frac{a_{11}}{a_{12}+z})}{a_{13} - a_9 - a_{10} z - \frac{a_{11}}{a_{12}+z}} \right\}. \tag{5}$$

see Figure 3. The surface C is S shaped with two fold curves: $F_{\pm} := \left\{ (x, y, z) \in C;\ z = \pm\sqrt{\frac{a_{11}}{a_{10}}} - a_{12} \right\}$.

As mentioned in the introduction the plane Π as well as the sets $z > 0$ and $z < 0$ are invariant for the flow. The MMOs observed by [6] are contained in the plane $z > 0$. The MMO trajectories make small oscillations near F_+, subsequently jump to the stable part of Π, follow it , crossing the instability line defined by the intersection of Π and C and subsequently follow the unstable part of Π. The passage along Π corresponds to a very simple delay phenomenon; since Π is always invariant the amount of time spent by the trajectory near the unstable part of Π is determined by the balance of attraction and expansion along Π. The role of Π is similar to the role of the invariant line in the article of Pokrovskii *et. al.* [23].

Note that the dynamics would be different if the invariance of Π was broken for $\varepsilon > 0$ as a delay phenomenon would occur only near discrete parameter values (due to the passage near a canard trajectory), see [18]. An analogous effect can be expected in systems with symmetry thus pointing to a significant change of the dynamics that can be brought about by the presence of symmetry in slow-fast systems.

An additional feature of the global return for system (1)–(3) is that the dynamics is mainly in the x direction, so that the system returns to F_+ with approximately the same values of y. An interesting situation happens near F_+, where the trajectories are attracted to the vicinity of the saddle point p_s and the rotations occur in the vicinity of p_s (see Figure 3).

3. Numerical bifurcation analysis of the model

The numerical bifurcation analysis of system (1)–(3) in parameter a_5 was performed with AUTO [10]; the results are presented in Figure 1. Panel (a) shows families of stationary and periodic attractors

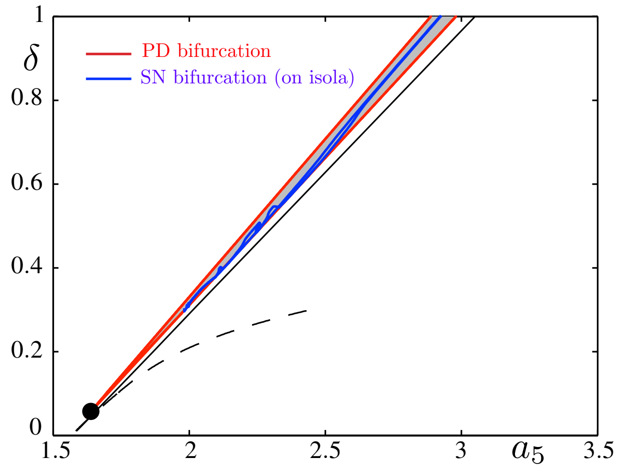

Figure 2: Locus of *PD* bifurcations (red curve) in the (a_5, δ)-plane computed using a numerical continuation routine, superimposed onto the diagram shown in [6] figure 4 and computed in the same plane. The curve of *PD* clearly agrees with the boundary of the region where MMO dynamics has been observed by direct simulation of the mode.

of the system as a function of a_5 in the interval $[1.96, 2.03]$, where interesting dynamics exists. These computations reveal that the unique non trivial ($z \neq 0$) equilibrium destabilizes via a Hopf bifurcation (H) at $a_5 \approx 2.025278$; this value depends on ε and is rather close to the value $a_5 = 1.987$ chosen in Figure 3. A pair of period-doubling bifurcations (*PD*) are detected along the branch of limit cycles born at the Hopf bifurcation and they organize the stability of this branch. When switching to the branch of period-doubled cycles, we find another two *PD* bifurcations. These *PD* bifurcations are likely to be organized in cascades and generate chaotic dynamics in a certain band of parameter values. Along each computed branch of periodic solution – period one, two and four are shown in Figure 1, many more are expected to exist in this parameter region – an explosion takes place by which small cycles (small period-2 cycles, small period-4 cycles, etc.) grow into large amplitude relaxation cycles (1^1 MMO, 1^3 MMO, etc.). Furthermore, certain MMO solutions (like the one shown in figure 3) happen to lie along closed curves in parameter space, also referred to as *isolas*; we show one such isola in figure 1 along which MMOs have a 1^2 pattern of oscillation. Note that the relaxation cycles and the relaxation loop of MMOs are possible due to the second branch of the *critical manifold* C of the system, that is, the plane $\{z = 0\}$, which is attracting in the x-interval where the folded sheet of C is unstable; please refer to section 4 for more details about C. This double canard effect — canard explosion giving a canard segment around a fold point of the critical manifold, and delayed-exchange of stability giving a second canard segment near a non-fold non-hyperbolic point of the critical manifold — has already been reported, and termed *canard doublet*, in a population dynamics context with the famous Lotka-Volterra equations; see [23]. This phenomenon is illustrated in Figure 1 (c) where a period-doubled cycle (blue) and a 1^1 MMO (red), computed along the period two branch displayed in panel (a) for very near values of a_5, are shown on top of the critical manifold (black). The explosive character of the periodic branches of solutions is only clearly observable for small enough ε; Figure 1 (b) presents the branch of period one solutions computed for three decreasing values of ε: 1e−03 (blue), 5e−04 (cyan) and 1e−04 (magenta). Considering the narrow a_5-interval on the horizontal axis, this panel gives a good numerical evidence that the branch develops a nearly vertical segment as ε gets closer to the singular limit.

When following the right-most *PD* bifurcation of Figure 1 in two parameters, namely a_5 and δ, we find a (red) curve in this two-parameter plane that agrees well with the boundary of the region of MMO dynamics computed by direct simulation in [6] (figure 4). A comparison between both computation is presented in figure 2. This suggests that the period-doubling bifurcations play an important role in the generation of mixed-mode dynamics in this model, as we will confirm in section 4. We also show a (blue) curve of saddle node bifurcation of cycles on isolas, namely, we continued in two parameter both *SN* bifurcations detected on the isola shown in Figure 1 (a). The results indicates that this family of isolas of MMOs stays, in the (a_5, δ) inside the curve of *PD* bifurcations; this gives an additional numerical

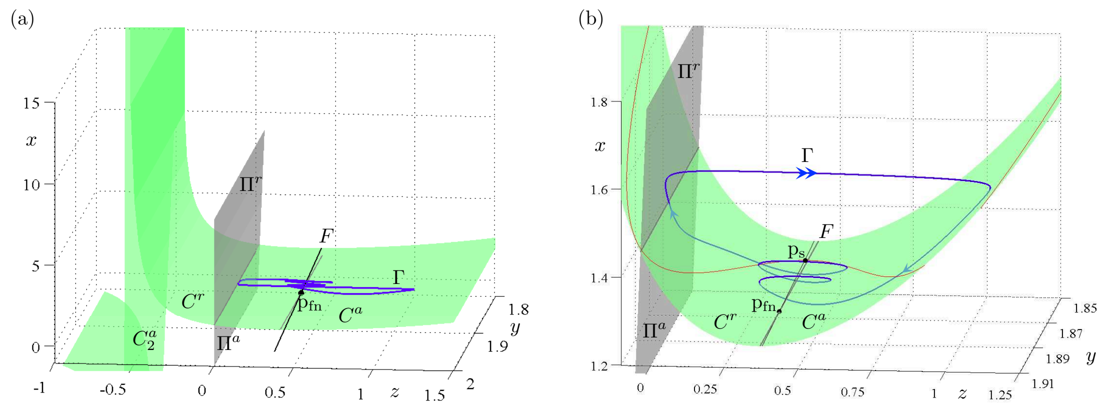

Figure 3: MMO of system (1)–(3) together with the critical manifold $C \cup \Pi$, formed by two components, each component having attracting and repelling submanifolds. The black dots are the folded node $\mathrm{p_{fn}}$ and the saddle-focus equilibrium $\mathrm{p_s}$ of the system; the red curve is the non-fold component of the y-nullcline of the DRS; the second black curve is the z-nullcline of the DRS. Panel (a) is an enlarged view of panel (b) that allows to see the second attracting sheet of C.

evidence that the MMO dynamics is confined, in this two-parameter plane, to the narrow band already shown in [6]. Therefore, from this bifurcation analysis we can conclude that the existence of mixed-mode dynamics in this model is related to period-doubling bifurcations followed, for ε small enough, by canard explosions.

4. Slow-fast analysis of the model – local dynamics near FS_+.

We will focus only on the fold curve $F_+ = F$ since the MMOs oscillate around it; see figure 3. We let $\alpha = \sqrt{\frac{a_{11}}{a_{10}}} - a_{12}$; we will use α later on to show that, for the chosen set of parameters, system (1)–(3) falls into the singular Hopf bifurcation scenario as far as the origin of MMOs is concerned.

We consider a parameter regime already studied in [6], namely, we fix: $a_5 = 1.987$ and $\delta = 0.3$ as in figure 3 (e)-(f) of [6]. The periodic attractor of the system for these parameter values is an MMO of pattern 1^2, i.e., with one large-amplitude oscillation (LAO) and two small-amplitude oscillations (SAOs).

The analysis of the desingularized reduced system (DRS)

$$\delta\dot{y} = \varphi'(z)(a_5\varphi(z) - (a_6(\varphi(z) - a_7)^2 + a_8 + \delta a_1)y, \tag{6}$$

$$\dot{z} = a_1 y - a_2\varphi(z) - a_3\frac{\varphi(z)z}{\varphi(z) + a_4}. \tag{7}$$

shows that system (1)–(3) possesses a *folded node*, that is, a node equilibrium of the desingularized reduced system (6)–(7) that lies on the fold curve F. Hence, at a folded node one has $\varphi'(z) = 0$, or equivalently $z_{\mathrm{fn}} = \alpha = \sqrt{\frac{a_{11}}{a_{10}}} - a_{12}$. Finally, we find the following expressions for the coordinates of the folded node (we verify numerically that it is indeed a node)

$$x_{\mathrm{fn}} = \varphi(\alpha) = \frac{a_4(a_9 + 2\sqrt{a_{10}a_{11}} - a_{10}a_{12})}{a_{13} - (a_9 + 2\sqrt{a_{10}a_{11}} - a_{10}a_{12})} \tag{8}$$

$$y_{\mathrm{fn}} = \frac{x_{\mathrm{fn}}}{a_1}(a_2 + a_3\frac{z}{x_{\mathrm{fn}} + a_4}) \tag{9}$$

$$z_{\mathrm{fn}} = \alpha. \tag{10}$$

Through visualization (see figure 3), we realize that the folded node is not located at the center of the SAOs of the MMO we consider; this gives the intuition that the dynamics cannot be fully understood by invoking folded node theory.

We argue that this is due to the fact that the system is close to a singular Hopf bifurcation. For all a_5, we can prove, by standard approach [25], that system (1)–(3) has a unique folded singularity given by (8)–(10). We can transform the coordinates so that (1)–(3) becomes:

$$\begin{aligned} \dot{x} &= \mu + Ax + Bz + \text{ h.o.t,} && (11)\\ \delta\dot{y} &= x - y + \text{ h.o.t,} && (12)\\ \varepsilon\dot{z} &= (-x + \phi(z))(z + \alpha), && (13) \end{aligned}$$

where μ, A and B are functions of the parameters $a_1, \ldots, a_{13}$ and δ. To achieve this transformation we first replace x by $x/(a_4 + x)$, then translate the variables to the folded node point and rescale. For each $\mu > 0$ the origin is a folded node point and $\mu = 0$ corresponds to a singular Hopf bifurcation. The value of a_5 corresponding to $\mu = 0$ is $a_5 \approx 2.030596282$. We found this value by expanding the vector field about the folded node and calculating the value of a_5 for which the resulting Taylor expansion has its constant term vanishing, which indeed corresponds to $\mu = 0$ in (11)–(13). Note that the value of the Hopf bifurcation computed with Auto is $a_5 \approx 2.0252772146$ for $\varepsilon = 1\text{e}{-03}$, $a_5 \approx 2.0279173803$ for $\varepsilon = 5\text{e}{-04}$, and $a_5 \approx 2.0300574958$ for $\varepsilon = 1\text{e}{-04}$.

It is known [16] that for singular Hopf bifurcation there is a center manifold with Hopf type dynamics near the folded singularity. For $\mu > 0$ but very small this center manifold corresponds to a saddle-focus point with a strongly stable real eigenvalue and a weakly unstable center direction. The trajectories passing near the folded singularity are attracted to the unstable manifold (center manifold) of the saddle point and follow the dynamics on it. Therefore the SAOs are close to the saddle focus equilibrium rather than stay near the folded singularity.

The transition between the center manifold and the structure of slow manifolds further away from the fold line is the origin of chaotic dynamics. By this mechanism simple periodic orbits undergo a period doubling cascade en route to chaos. Subsequently, complicated periodic orbits undergo canard explosions on one of their loops, growing to MMOs. This is the mechanism of the generation of MMO orbits (which is till not completely understood, see [16] and [17]. In Figure 1 we show a transition from a period doubled orbit to a 1^1 MMO by way of a canard explosion.

The maximal number of small oscillations in a MMO generated from a folded node can be computed from

$$s_{\max} = [\Psi(\mu)]\,, \qquad (14)$$

where $[\cdot]$ denotes the integer part and $\Psi(\mu)$ is a smooth function satisfying $\Psi(\mu) = O(1/\mu)$, see [27, 26]. Applying this to the case $a_5 = 1.987, \delta = 0.3$ yields $s_{\max} = 27$, substantially above the actual value $s = 2$. This also indicates that the folded node scenario is of limited relevance here.

5. Conclusion

In this paper, we completed the analysis of MMOs done in [6] for the forest pest model (1)–(3). Namely, we showed that this model provides a good example where the generating mechanism is the singular Hopf bifurcation and not the presence of a folded singularity. This is a good application of the recent theory developed, in particular, in [16]. Indeed, there is clearly a folded node in the model but its role is not decisive in shaping and organising the MMOs, hence the mismatch between the number of SAOs found by applying folded node theory [7] compared to the observed number.

By looking closely at the bifurcation structure of the model, in particular, the location of the folded singularity, the location of the saddle-focus equilibrium of the full system and the magnitude of the real part of its eigenvalues, one can relate the situation observed in the forest pest model for the chosen parameter set to the "Singular Hopf bifurcation scenario" as opposed to the "folded node / folded saddle-node" scenario. This is in light of the recent work done in [7, 16, 17, 20]. In particular, the role of period-doubling bifurcations in the mixed-mode dynamics in a singular Hopf normal form was pointed in [17], in link with canard explosion phenomena. We show, by means of numerical continuation, that the presence of MMOs in system (1)–(3), owes (for small enough ε) to the explosion of small amplitude period-$2n$ ($n \in \mathbb{N}$) cycles that are born along a cascade of period-doubling bifurcations. This cascade involves a small-amplitude chaotic attractor. There are also period-$(2n+1)$ orbits lying on isolas and that change their LAO profile through period-doubling bifurcations as well.

Finally, future work include looking at the family of isolas in parameter space, how MMOs living on them are organized, how such families are created and destroyed; this involve numerical as well as theoretical questions that we are planning to address in a follow-up paper.

References

[1] M. Ya. Antonovsky, R. A. Fleming, Yu. A. Kuznetsov, and W. C. Clark. *Forest-pest interaction dynamics: The simplest mathematical models*. Theor. Popul. Biol. **37**:343–367, 1990.

[2] E. Benoît, J.-L. Callot, F. Diener, and M. Diener. *Chasse au canard*. Collect. Math. **3**:37–119, 1981.

[3] E. Benoît. *Canards et enlacements*. Inst. Hautes Études Sci. Publ. Math. **72**:63–91, 1990.

[4] A. A. Berryman, N. C. Stenseth, and A. S. Isaev. *Natural regulation of herbivorous forest insect populations*. Oecologia **71**:174–184, 1987.

[5] M. Brøns, and K. Bar-Eli. *Asymptotic analysis of canards in the EOE equations and the role of the inflection line*. Proc. R. Soc. Lond. A **445**:305–322, 1994.

[6] M. Brøns, and R. Kaasen. *Canards and mixed-mode oscillations in a forest pest model*. Theor. Popul. Biol. **77**:238–242, 2010.

[7] M. Brøns, M. Krupa, and M. Wechselberger. *Mixed mode oscillations due to the generalized canard phenomenon*. In *Bifurcation theory and spatio-temporal pattern formation*, volume 49 of Fields Inst. Commun., pages 39–63. Amer. Math. Soc., Providence, RI, 2006.

[8] Buřič, L., Klíč, A. and Purmová, L. *Canard solutions and travelling waves in the spruce budworm population model*. Appl. Math. Comput. **43**:1039–1051, 2006.

[9] M. Desroches, B. Krauskopf, and H. M. Osinga. *Mixed-mode oscillations and slow manifolds in the self-coupled FitzHugh-Nagumo system*. Chaos **18**(1):015107, 2008.

[10] E. J. Doedel, R. C. Paffenroth, A. R. Champneys, T. F. Fairgrieve, Yu. A. Kuznetsov, B. E. Oldeman, B. Sandstede, and X. J. Wang. *AUTO-07P: Continuation and bifurcation software for ordinary differential equations*. Available at the following URL: `http://indy.cs.concordia.ca/auto`, 2007.

[11] N. Fenichel. *Geometric singular perturbation theory*. J. Differential Equations **31**:53-98, 1979.

[12] A. Gragnani, M. Gatto, and S. Rinaldi. *Acidic deposition, plant pests, and the fate of forest ecosystems*. Theor. Popul. Biol. **54**:257–269, 1998.

[13] J. Guckenheimer, K. Hoffman, and W. Weckesser. *Numerical computation of canards* Int. J. Bifurcations and Chaos **10**(12):2669–2687, 2000.

[14] J. Guckenheimer, and R. Haiduc. *Canards at folded nodes* Mosc. Math. J. **5**(1):91–103, 2005.

[15] J. Guckenheimer. *Return maps of folded nodes and folded saddle-nodes* Chaos **18**(1), 015108, 2008.

[16] J. Guckenheimer. *Singular Hopf bifurcation in systems with two slow variables* SIAM J. Appl. Dyn. Syst. **7**(4):1355–1377, 2008.

[17] J. Guckenheimer, and P. Meerkamp. *Unfolding of singular Hopf bifurcation* preprint, July 2011.

[18] M. Krupa and P. Szmolyan. Transcritical and pitchfork singularities of critical manifolds. Nonlinearity **14**, 1473–1491, 2001.

[19] D. R. Kucera, and P. W. Orr. *Spruce Budworm in the Eastern United States*. Forest Insect & Disease Leaflet 160. U.S. Department of Agriculture Forest service. `http://na.fs.fed.us/spfo/pubs/fidls/sbw/budworm.htm`, 1981.

[20] M. Krupa, and M. Wechselberger. *Local analysis near a folded saddle-node singularity*, J. Differential Equations **248**(12):2841–2888, 2010.

[21] D. Ludwig, D. Jones, and C. S. Holling. *Qualitative analysis of insect outbreak systems:The spruce budworm and forest.* J. Anim. Ecol. **47**:315–332, 1978.

[22] S. Muratori, and S. Rinaldi. *Catastrophic bifurcations in a second-order dynamical system with application to acid rain and forest collapse.* Appl. Math. Modelling **13**:674–681, 1989.

[23] A. Pokrovskii, E. Shchepakina and V. Sobolev. *Canard doublet in a Lotka-Volterra type model.* J. Phys.: Conf. Ser. **138**: 012019, 2008.

[24] S. Rinaldi, and S. Muratori. *Limit cycles in slow-fast forest-pest models.* Theor. Popul. Biol. **41**:26–43, 1990.

[25] P. Szmolyan, and M. Wechselberger. *Canards in* $\mathbb{R}^3$. J. Differential Equations **177**(2):419–453, 2001.

[26] T. Vo, R. Bertram, J. Tabak, and M. Wechselberger. *Mixed mode oscillations as a mechanism for pseudo-plateau bursting.* J. Comput. Neurosci. **28**(3):443–458, 2010.

[27] M. Wechselberger. *Existence and bifurcation of canards in* $\mathbb{R}^3$ *in the case of a folded node.* SIAM J. Appl. Dyn. Syst. **4**(1):101–139, 2005.